DOI: 10.1002/ejic.200901057

Synthesis, Structures, and Properties of New Chalcogenide-Capped Octahedral Hexatechnetium(III) Complexes $[Tc_6S_8X_6]^{4-}$ (X = Br, I), $[Tc_6Se_8I_2]$, and $[Tc_6Te_{15}]$

Takashi Yoshimura,*[a] Takuya Ikai,[a] Yuji Tooyama,[a] Tsutomu Takayama,[b] Tsutomu Sekine,[c] Yasushi Kino,[d] Akira Kirishima,[e] Nobuaki Sato,[e] Toshiaki Mitsugashira,[f] Naruto Takahashi,[a] and Atsushi Shinohara[a]

Keywords: Technetium / Chalcogens / Cluster compounds / Cyclic voltammetry

Chalcogenide-capped octahedral hexatechnetium(III) complexes, $Cs_4[Tc_6S_8Br_6]\cdot CsBr$ (Cs_4[**1**]·CsBr) and $(PPh_4)_4[Tc_6S_8Br_6]$ {$(PPh_4)_4$[**1**]}, $(PPh_4)_4[Tc_6S_8I_6]$ {$(PPh_4)_4$[**2**]}, $[Tc_6Se_8I_2]$ ([**3**]), and $[Tc_6Te_{15}]$ ([**4**]) were synthesized. Single-crystal X-ray structural studies were carried out for Cs_4[**1**]·CsBr, [**3**], and [**4**]. Sulfide-capped octahedral hexatechnetium(III) clusters $[\mathbf{1}]^{4-}$ and $[\mathbf{2}]^{4-}$ are discrete complex anions, whereas the selenide- and telluride-capped hexatechnetium(III) complexes adopt extended polymeric structures. A cyclic voltammogram of $[\mathbf{1}]^{4-}$ in CH_3CN showed two one-electron redox waves: Tc_6(24e/23e) and Tc_6(23e/22e). The potential of the Tc_6(24e/23e) process is more positive than that of the Re_6(24e/23e) process for the hexarhenium analog $[Re_6S_8X_6]^{4-}$ (X = Br, I), whereas that of the Tc_6(23e/22e) process shifts to negative values compared to the potential of the Re_6(23e/22e) process. Thus, the Tc_6(23e) mixed-valence state is thermodynamically less stable than Re_6(23e).

Introduction

The octahedral hexanuclear complex having an M_6Q_8 core (Q = chalcogenide, halide) and six axial ligands is a well-known structure among metal cluster complexes (Figure 1). The chemistry of halide-capped hexamolybdenum(II) and hexatungsten(II) complexes and chalcogenide-capped hexarhenium(III) and mixed rhenium(III)–osmium(IV) complexes with 24 valence electrons (24e) have been well studied.[1–15] Such octahedral hexatechnetium complexes are still limited. Chalcogenide-capped octahedral hexatechnetium clusters, $[Tc_6Q_x]$ (Q = S, x = 12–14; Q = Se, x = 12–13), were firstly reported by Bronger et al.[16,17] Kryutchkov et al. reported a bromide-capped cluster $[Tc_6(\mu_3\text{-}Br)_5Br_6]^{2-}$ in which the eight capping sites were not fully occupied.[18–20] In this study, we report on several new chalcogenide-capped hexatechnetium(III) complexes that are expected to be the precursors for the synthesis of various hexatechnetium(III) complexes. We also report on the redox properties of the soluble discrete molecules $[Tc_6S_8X_6]^{4-}$ (X = Br, I). The redox potential of the Tc_6(24e/23e) process is more positive than that of the Re(24e/23e) process in the hexarhenium analog $[Re_6S_8X_6]^{4-}$ (X = Br, I). On the other hand, the potential of the Tc_6(23e/22e) process shifts to negative values as compared to the potential of the Re_6(23e/22e) process, which is the opposite of the tendency usually observed in Tc and Re complexes.

[a] Department of Chemistry, Graduate School of Science, Osaka University,
Toyonaka, Osaka 560-0043, Japan
Fax: +81-6-6850-5416
E-mail: tyoshi@chem.sci.osaka-u.ac.jp
[b] Department of Chemistry, Daido University,
Nagoya, Aichi 457-8530, Japan
[c] Center for the Advancement of Higher Education, Tohoku University,
Sendai, Miyagi 980-8576, Japan
[d] Department of Chemistry, Graduate School of Science, Tohoku University,
Sendai, Miyagi 980-8576, Japan
[e] Institute of Multidisciplinary Research for Advanced Materials, Tohoku University,
Sendai, Miyagi 980-8577, Japan
[f] International Research Center for Nuclear Materials Science, Institute for Materials Research, Tohoku University,
Oarai, Ibaraki 311-1313, Japan

Supporting information for this article is available on the WWW under http://dx.doi.org/10.1002/ejic.200901057.

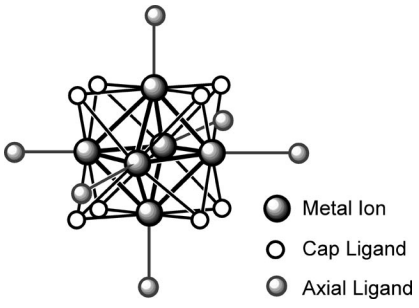

Figure 1. Octahedral hexanuclear complex.

Results and Discussion

Crystal Structures

Single-crystal X-ray structural analyses were carried out for three of the new complexes: $Cs_4[Tc_6S_8Br_6]\cdot CsBr$ (Cs_4[**1**]·CsBr), $[Tc_6Se_8I_2]$ ([**3**]), and $[Tc_6Te_{15}]$ ([**4**]). Selected bond lengths and angles are summarized in Table 1, and the crystallographic data are listed in Table 2. Figure 2 shows the complex anion of Cs_4[**1**]·CsBr. The six technetium atoms form a nearly regular octahedron with Tc–Tc–Tc angles of either 59.95(2)–60.10(3) or 90.000(5)°. The eight sulfur atoms cap each of the faces of the metal triangles. All of the six axial positions are occupied by bromine atoms. The four negative valence of the complex anion indicate that all of the Tc ions have a +3 oxidation state. The Tc–Tc distances [2.584(1)–2.588(1) Å] correspond to single bonds and are slightly shorter than those of the molecular hexatechnetium complexes that have axial sulfides $M_{10}[Tc_6S_{14}]$ [M = Cs, 2.627(3) Å; M = Rb, 2.633(3) Å]. The Tc–S bond lengths [2.377(2)–2.392(2) Å] are close to those of $M_{10}[Tc_6S_{14}]$ [M = Cs; 2.388(5) Å, M = Rb; 2.400(3) Å].[16] The Tc–Br bond length [2.570(1) Å] is similar to those of other technetium(III) complexes such as $[\{TcBr(2,2'\text{-bipyridine})_2\}_2(\mu\text{-O})]^{2+}$ [2.5665(7) Å][21] and $Tc(NS)(S_2CNEt_2)_2Br_2$ [2.5647(1)–2.595(1) Å].[22]

Figure 3 shows the structure of polymeric cluster [**3**] containing Tc_6Se_8 units. Eight selenium atoms cap the eight triangular faces of the hexatechnetium octahedron. Two of these eight capping selenides are connected to the axial sites of the neighboring hexanuclear core, and axial iodides also act as bridges between the hexatechnetium units, so that the complex becomes neutral. The Tc–Tc distances [2.609(1)–2.665(1) Å] and the Tc–Se distances [2.482(2)–2.509(1) Å], with the exception of Tc3–Se1, are similar to those of the reported selenide-coordinated hexatechnetium cluster $Cs_4Tc_6Se_{13}$.[16] The distances between Tc3 and μ_4-Se1 that are involved in the intercluster bridges [2.601(2) and 2.626(2) Å] are longer than those of the Tc–(μ_3-Se) bonds. The Tc–I bonds [2.774(1)–2.798(1) Å] are in the range of the data found in the hexanuclear trigonal prism $[\{Tc_6(\mu_2\text{-}I)_6I_6\}I_2]^{3-}$ [Tc–I(axial) 2.71(1) Å],[23] as well as in tetrameric $[Tc(CO)_3I]_4$ [av. 2.846(3) Å][24] and mononuclear $[Tc(CO)_5I]$ [2.807(1) Å].[25]

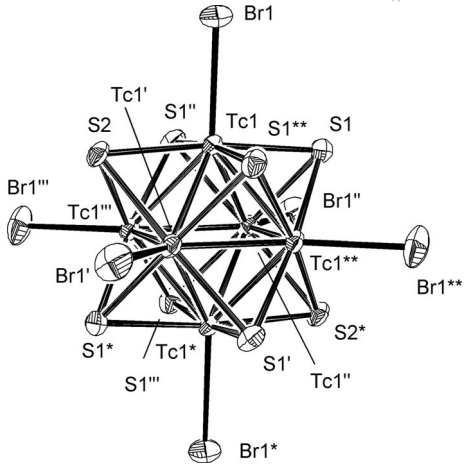

Figure 2. ORTEP drawing showing the complex anion of $Cs_4[Tc_6S_8Br_6]\cdot CsBr$ (Cs_4[**1**]·CsBr) and its numbering scheme.

The polymeric structure [**4**] is shown in Figure 4. Complex [**4**] is composed of Tc_6Te_8 and Te_7 clusters. All six axial Te atoms are provided by the μ_3-Te atoms of the Te_7 cluster. The six technetium atoms are arranged in a nearly regular octahedron. The Tc–Tc distances [2.677(2)–2.695(2) Å] are ca. 0.06 Å longer than those in selenide-capped complex [**3**], and longer by ca. 0.1 Å than those in sulfide-capped complex [**1**]$^{4-}$. The Tc–Te(cap) distances [2.668(2)–2.693(2) Å] are ca. 0.3 and 0.18 Å longer than the Tc–S distances in [**1**]$^{4-}$ and the Tc–Se distances in [**3**], respectively. The Tc–Te(axial) distances [2.700(2)–2.732(2) Å] are somewhat longer than the Tc–Te(cap) distances. It seems that the capping telluride is more strongly bound to the technetium atom

Table 1. Selected bond lengths [Å] and angles [°] of Cs_4[**1**]·CsBr, [**3**], and [**4**].

	Cs_4[**1**]·CsBr	[**3**]	[**4**]
Tc–Tc	2.584(1)–2.588(1) av. 2.586(2)	2.609(1)–2.665(1) av. 2.629(2)	2.677(2)–2.695(2) av. 2.689(5)
Tc–Q$^{c[a]}$	2.377(2)–2.392(2) av. 2.386(6)	2.482(2)–2.626(2) av. 2.505(5)	2.668(2)–2.693(2) av. 2.678(7)
Tc–Q$^{a[b]}$		2.601(2)	2.700(2)–2.732(2) av. 2.712(3)
Tc–X	2.570(1)	2.774(1)–2.798(1) av. 2.786(1)	
Tc–Tc–Tc	59.95(2)–60.10(3) av. 60.00(7)	59.20(3)–61.34(3) av. 60.0(1)	59.68(6)–60.21(5) av. 60.0(1)
Tc–Tc–Tc	90.000(5)	89.14(4)–90.86(4) av. 90.0(1)	89.82(6)–90.18(6) av. 90.0(1)
Tc–Q^{c}–Tc$^{[a]}$	65.48(7)–65.78(7) av. 65.6(1)	61.09(4)–64.42(4) av. 63.3(1)	59.96(5)–60.57(5) av. 60.3(2)
Q^{c}–Tc–Q$^{c[a]}$	89.55(4)–90.03(4) av. 89.8(2)	86.05(5)–93.51(5) av. 90.0(2)	89.43(6)–90.65(6) av. 90.2(2)
Q^{c}–Tc–Q$^{c[a]}$	173.02(8)–173.04(7) av. 173.03(8)	173.95(5)–176.50(5) av. 174.9(1)	179.02(7)–179.70(7) av. 179.4(2)

[a] Q^{c}: capping chalcogenide. [b] Q^{a}: axial chalcogenide.

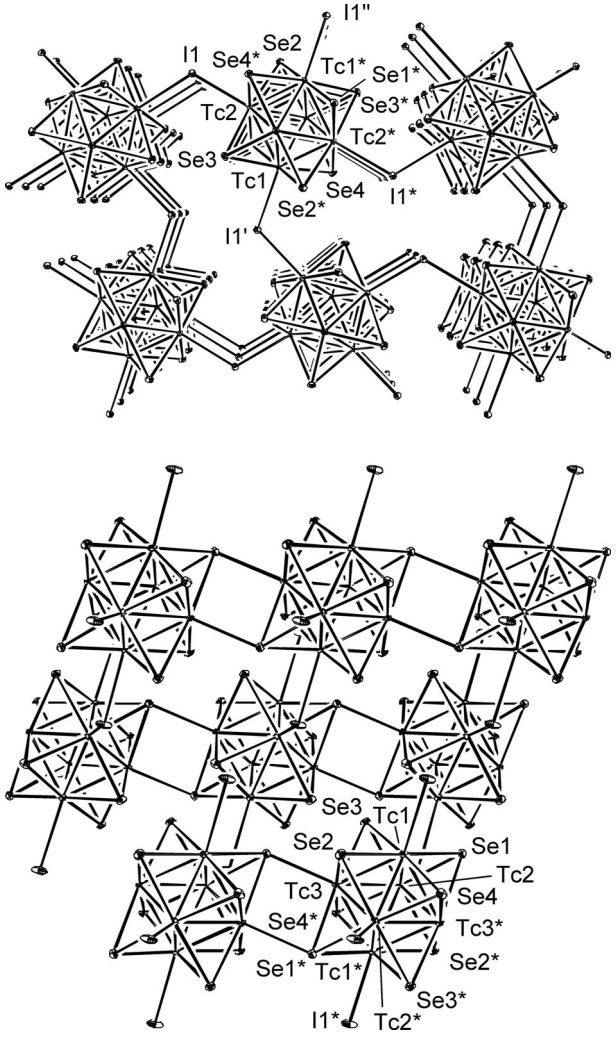

Figure 3. ORTEP drawings showing part of the structure [top view (top) and side view (bottom)] of $[Tc_6Se_8I_2]$ ([**3**]) and its numbering scheme.

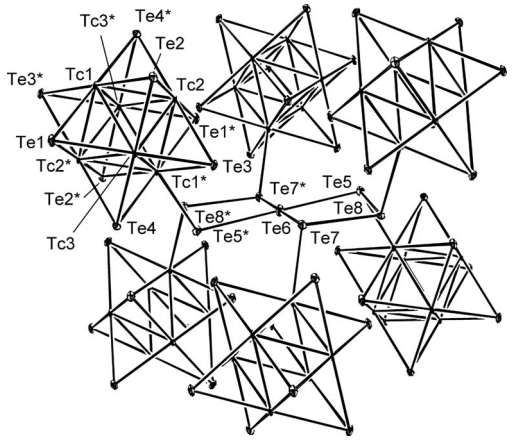

Figure 4. ORTEP drawing showing part of structure of $[Tc_6Te_{15}]$ ([**4**]) and its numbering scheme.

than the axial telluride. The Te_7 cluster takes a corner-shared birhomboidal structure and is composed of six μ_3-Te atoms and one μ_4-Te atom. All six μ_3-Te atoms in the Te_7 cluster coordinate to the axial sites of the hexatechnetium(III) telluride units to complete a 3D polymeric structure. A Te_7 cluster similar to the present one was previously found in Re_6Te_{15}[26] and has similar structural features to the one in [**4**], as described below. The μ_4-Te atom is located at the corner of the two rhombs to give a square-planar geometry [*cis* Te–Te–Te 88.31(4) and 91.69(4)°, *trans* Te–Te–Te 180.0°]. The bond angles around the μ_3-Te atoms are Te–Te–Te 84.06(4), 85.40(4), and 97.96(5)°. The Te–Te distances span a range of 2.837(2)–3.023(1) Å. These distances are classified into two groups. Shorter Te–Te distances are found between individual μ_3-Te atoms [Te5–Te8 2.877(2) Å and Te7–Te8 2.840(2) Å], and longer ones are found between the μ_3- and μ_4-Te atoms [Te5–Te6 3.023(1) Å and Te6–Te7 2.987(1) Å].

It should be noted that the structural features of the complexes of $[Tc_6S_8Br_6]^{4-}$ and $[Tc_6Te_{15}]$ complexes that have hexarhenium analogs are similar to those of the hexarhenium(III) cluster cores. The Tc–Tc distances are very similar to the Re–Re distances for $[Re_6S_8Br_6]^{4-}$ [2.596(3),[27] 2.594(7),[27] 2.5927(9),[28] 2.590(1),[29] 2.587(1)–2.590(6) Å],[30] and $[Re_6Te_{15}]$ (2.679 Å).[26]

Syntheses

The chalcogenide-capped hexatechnetium(III) clusters were formed by high-temperature reactions. The preparation methods for hexatechnetium(III) clusters in this study were almost similar to those for the hexarhenium(III) clusters, although the reaction volume for the hexatechnetium(III) complexes was much smaller than that used for hexarhenium complexes in the literature.[26,27]

The reaction of a stoichiometric ratio of elemental technetium, sulfur, and halogen with an excess amount of cesium halide at 850 °C, followed by slow cooling to room temperature, gave an orange crystalline solid together with colorless crystals of unreacted cesium halide. This orange crystalline mixture was dissolved in acid or water to give an orange solution. Orange cesium or tetraphenylphosphonium salts of $[Tc_6S_8X_6]^{4-}$ (X = Br; $[\mathbf{1}]^{4-}$, X = I; $[\mathbf{2}]^{4-}$) were isolated as pure products in reasonable yields by the addition of the corresponding cations to the solution. The UV/Vis spectral features resembled each other: both $[\mathbf{1}]^{4-}$ and $[\mathbf{2}]^{4-}$ exhibited a peak and a shoulder in the 300–400 nm region. The band and shoulder for $(PPh_4)_4[\mathbf{1}]$ in CH_3CN were observed at 344 and 320 nm, respectively. These were shown at a somewhat shorter wavelength in an aqueous solution of the cesium salt $Cs_4[\mathbf{1}]\cdot CsBr$, that is, at 335 and 315 nm, respectively. For $(PPh_4)_4[\mathbf{2}]$, the bands observed in CH_3CN at 399 and 355 nm, respectively, were considerably redshifted.

The selenide-capped complex was obtained as a metallic insoluble solid under the reaction condition similar to those used to synthesize the sulfide-capped complex. The X-ray fluorescence spectrum showed that the product contains Tc, Se, and I. Single-crystal X-ray analysis showed that it had a 3D polymeric structure. The X-ray powder pattern was in agreement with the pattern calculated from the X-ray structure obtained from single-crystal X-ray analysis.

The reaction of Tc, Se, and Br_2 with CsBr also gave an insoluble metallic product (see the Supporting Information). Single-crystal X-ray analysis revealed that this product contained $Cs_2[Tc_6Se_8Br_4]$ (Figure S1, Supporting Information). In the X-ray powder pattern, the positions of the intense signals were similar to those of the simulated signals, but their intensities were different from those of the simulated signals. Thus, it was concluded that an unidentified hexatechnetium polymeric structure may be included.

The sulfide- and selenide-capped hexatechnetium clusters were obtained as discrete molecules and linkage polymeric complexes, respectively. Although we adopted similar experimental conditions such as the ratio of the reactants and the reaction temperature, it is still premature to conclude that the difference in the bonding modes came from sulfide and selenide, as in the case of hexarhenium complexes, the linkage modes are easily changed depending on the reaction conditions.[7,10] Various linkage modes as seen in hexarhenium chemistry may be also found in the sulfide- and selenide-capped hexatechnetium complexes by changing the reaction conditions.

Metallic-colored, telluride-capped octahedral hexatechnetium(III) clusters were obtained from the reaction of elemental technetium with an excess amount of tellurium at 900 °C, followed by slow cooling to room temperature. The single crystals were obtained by manipulative separation from unreacted telluride. After confirmation by the X-ray fluorescence spectra, which showed Tc and Te were contained in this solid, the extended structure of the complex bridged by the Te_7 cluster was determined by single-crystal X-ray analysis. The X-ray powder pattern was in agreement with the pattern calculated from the X-ray structure obtained from single-crystal X-ray analysis.

Electrochemical Properties

Electrochemical properties of the hexatechnetium(III) complexes $[Tc_6S_8X_6]^{4-}$ (X = Br, I) were investigated by cyclic voltammetry in a 0.1 M Bu_4NPF_6/CH_3CN solution. A cyclic voltammogram of $[\mathbf{1}]^{4-}$ is shown in Figure 5. Two irreversible oxidation waves were observed at E_p = +0.77 and +1.05 V. When the scan sweep returned before the second oxidation step, the first redox wave became reversible at $E_{1/2}$ = +0.75 V. These redox waves were assigned to the Tc_6(24e/23e) and Tc_6(23e/22e) processes, respectively, because the peak intensities were almost comparable to those of the Re_6(24e/23e) and Re_6(23e/22e) processes of $[Re_6S_8X_6]^{4-}$ (X = Cl, Br) at the same concentration. The cyclic voltammogram for $[\mathbf{2}]^{4-}$ showed a one-electron irreversible oxidation wave at E_p = +0.50 V vs. Ag/AgCl. In the Re_6S_8 complexes, $[Re_6S_8X_6]^{4-}$ (X = Cl, Br, I) in 0.1 M Bu_4NPF_6/CH_3CN showed a reversible one-electron redox wave [Re_6(24e/23e)] at $E_{1/2}$ = +0.31, +0.33, and +0.36 V vs. Ag/AgCl, respectively.[10,27,31,32] Here, the differences in the redox potentials among the three different terminal halide complexes are small. The differences in the corresponding redox processes are more substantial for the hexatechnetium complexes. The positive shift in the potential of the Tc_6(24e/23e) process in $[\mathbf{1}]^{4-}$ as compared to that of $[\mathbf{2}]^{4-}$ may be attributed to the greater electron-donating properties of the terminal I^- relative to those of Br^-. Therefore, the substantial difference in the redox potentials of the Tc_6(24e/23e) process between $[\mathbf{1}]^{4-}$ and $[\mathbf{2}]^{4-}$ suggests that the HOMO levels of the Tc_6S_8 core have a higher axial halide characteristic. The Re_6(23e/22e) process was also observed in $[Re_6S_8X_6]^{4-}$ (X = Cl, Br) at $E_{1/2}$ = +1.17 V (quasi-reversible) for X = Cl and at E_p = +1.15 V (irreversible) for X = Br. The second oxidation of the hexarhenium complex with terminal iodide was observed at ca. +1.0 V as an irreversible wave. However, iodide oxidation waves are expected to occur in this potential region and further discussion may not be appropriate. The redox potentials for the +3 and +4 oxidation states were compared for several mononuclear Tc and Re complexes. The redox potentials of technetium complexes are more positive than those of the isomorphic rhenium complexes: $\Delta[Tc_2(III/IV) - Re_2(III/IV)]$ = +0.075–0.34 V.[33–37] A similar positive shift was also found in μ-oxido bridging dinuclear complexes {$\Delta[Tc_2(III,III/III,IV) - Re_2(III,III/III,IV)]$ = +0.43 V,[21,38] $\Delta[Tc_2(III,IV/IV,IV) - Re_2(III,IV/IV,IV)]$ = +0.43 V}.[21,38] These positive shifts are also found in hexanuclear complexes. For both $[\mathbf{1}]^{4-}$ and $[\mathbf{2}]^{4-}$, the oxidation potential of the Tc_6(24e/23e) process is more positive than that of the Re_6(24e/23e) process; the extent of the shift is +0.4 V for the axial bromide and +0.17 V for the axial iodide complexes. The tendency of a positive shift in the redox potential has been shown in $[M_6(\mu_3\text{-}Cl)_8Cl_6]^{2-}$ (M = Mo, W), in which the difference of redox potentials between Mo_6(24e/23e) and W_6(24e/23e) is +0.46 V.[39] It should be noted that the difference in the second oxidation steps {$\Delta[Tc_6$(23e/22e) – Re_6(23e/22e)] = –0.10 V} of the hexanuclear complexes with axial bromide ligands is small and even in the opposite direction. It may be that the oxidation states involving the second oxidation process contain a much higher contribution from the terminal halide ligands and that the influence from the different metal centers is obscured.

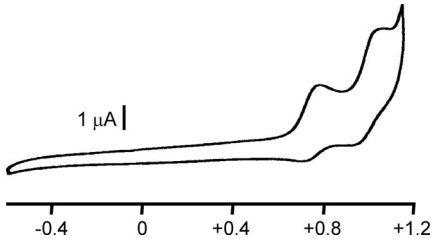

Figure 5. Cyclic voltammogram of $(PPh_4)_4[Tc_6S_8Br_6]$ in 0.1 M $(Bu_4N)PF_6/CH_3CN$ solution. Scan rate = 100 mV s^{-1}.

Conclusions

Chalcogenide-capped octahedral hexatechnetium(III) clusters, discrete molecules $[Tc_6S_8X_6]^{4-}$ (X = Br, I) and polymeric complexes $[Tc_6Se_8I_2]$, and the first example of octahedral hexatechnetium(III) telluride $[Tc_6Te_{15}]$ were synthesized, and three of them were structurally characterized.

The molecular complex $[Tc_6S_8Br_6]^{4-}$ showed two one-electron redox waves, which were assigned to the hexatechnetium cluster core. The potential of the Tc_6(24e/23e) process was more positively shifted than that of the Re_6(24e/23e) process for the isomorphic hexarhenium complex, following the normal tendency between second- and third-row transition-metal complexes. The second oxidation wave [Tc_6(23e/22e)] showed a more negative shift than the corresponding value of the hexarhenium analog. As a result, the Tc_6(23e) mixed-valence state was found to be thermodynamically less stable than the corresponding hexarhenium complex. Sulfide-capped octahedral hexarhenium(III) clusters having axial halides $[Re_6S_8X_6]^{3-\text{ or }4-}$ and $[Re_6Te_{15}]$ are known to be good precursors for preparing various hexarhenium(III) clusters by the substitution of axial and capping ligands.[7,9,10] Thus, the hexatechnetium(III) clusters in this study also show promise as good starting materials for various hexatechnetium complexes. Work is now in progress to synthesize various derivatives by substitution reactions of the hexatechnetium(III) clusters.

Experimental Section

Materials: The isotope 99-technetium metal was kindly given to us by Dr. K. Minato of Japan Atomic Energy Agency as a gift and was used in the syntheses of all the technetium complexes described in this paper. *CAUTION:* The isotope 99-technetium is a low-energy β-emitter with a half-life of 2.11×10^5 y and E_{max} = 290 keV. The vessels for high-temperature reactions were silica ampoules (id × od × l = 8 × 10 × 100 mm). Acetonitrile was distilled from CaH_2 under a N_2 atmosphere. As the supporting electrolyte, $(Bu_4N)PF_6$ was recrystallized (2×) from ethanol.

Preparation of $Cs_4[Tc_6S_8Br_6]$·CsBr (Cs_4[1]·CsBr) and $(PPh_4)_4$-$[Tc_6S_8Br_6]$ {$(PPh_4)_4$[1]}: Technetium metal (19.5 mg, 0.197 mmol), sulfur (8.5 mg, 0.27 mmol), bromine (5.3 mg, 0.033 mmol), and CsBr (50.0 mg, 0.231 mmol) were charged into a silica ampoule. The ampoule was cooled with liquid nitrogen and then sealed under static vacuum. The ampoule was shaken to mix the contents, heated to 850 °C at a rate of 2 °C min^{-1}, maintained at 850 °C for 100 h, cooled to 400 °C at a rate of 0.2 °C min^{-1}, and then left at room temperature. A crude product containing orange crystals and a colorless solid was obtained. A portion of this crude product (32.2 mg) was dissolved in 1 M hydrobromic acid (5 mL) and filtered. Cesium bromide (100 mg, 0.469 mmol) in water (2 mL) was added to this solution, and the reaction mixture was allowed to stand for several days to give orange cesium salt crystals. These crystals were collected by filtration and dried in air. Yield of Cs_4[1]·CsBr: calcd. 20.7 mg (77%). $Cs_5Tc_6S_8Br_7$ (2074.38): calcd. Tc 28.6; found. Tc 29.0. UV/Vis (H_2O): λ (ε, M^{-1} cm^{-1}) = 335 (sh., 8800), 315 (9500), 251 (sh., 33900), 224 (60800) nm. A single crystal suitable for X-ray analysis was selected from the obtained crystals. The tetraphenylphosphonium salt was obtained by using tetraphenylphosphonium bromide in place of cesium bromide. A solution of tetraphenylphosphonium bromide (30 mg, 0.072 mmol) in methanol (5 mL) was added to the crude product (27.6 mg) in 1 M hydrobromic acid (5 mL). The orange precipitate was collected by filtration, washed with methanol, and then dried in air. Yield of $(PPh_4)_4$[**1**]: 25.9 mg (87%). $C_{96}H_{80}Br_6P_4S_8Tc_6$ (2687.54): calcd. C 42.9, H 3.00, Tc 22.1; found C 42.7, H 3.14, Tc 22.3. UV/Vis (CH_3CN): λ (ε, M^{-1} cm^{-1}) = 344 (sh., 11500), 320 (11800), 258 (57400), 227 (174000) nm.

$(PPh_4)_4[Tc_6S_8I_6]$ {$(PPh_4)_4$[2]}: Technetium metal (21.2 mg, 0.214 mmol), elemental sulfur (9.4 mg, 0.293 mmol), iodine (9.2 mg, 0.036 mmol), and cesium iodide (84.0 mg, 0.323 mmol) were charged into a silica ampoule. The ampoule was cooled with liquid nitrogen and then sealed under static vacuum. The ampoule was shaken to mix the contents, heated to 850 °C at a rate of 2 °C min^{-1}, maintained at 850 °C for 100 h, cooled to 400 °C at a rate of 0.2 °C min^{-1}, and then left at room temperature. A crude product containing yellow-orange microcrystals and a colorless solid was obtained. A portion of this crude product (23.6 mg) was dissolved in 0.1 M hydroiodic acid (10 mL), and then tetraphenylphosphonium iodide (23 mg, 0.049 mmol) in methanol (3 mL) was added to the reaction mixture. The deposited precipitate was collected by filtration, washed with methanol, and then dried in air. Yield of $(PPh_4)_4$[**2**]: 18.0 mg (88%). $C_{96}H_{80}I_6P_4S_8Tc_6$ (2969.54): calcd. C 38.8, H 2.72, Tc 20.0; found C 39.2, H 2.83, Tc 20.2. UV/Vis (CH_3CN): λ (ε, M^{-1} cm^{-1}) = 399 (sh., 14900), 355 (20000), 286 (sh., 51000), 276 (60200), 269 (58200), 225 (sh., 212000) nm.

$[Tc_6Se_8I_2]$ ([3]): Technetium metal (20.4 mg, 0.206 mmol), elemental selenium (21.5 mg, 0.272 mmol), iodine (8.6 mg, 0.034 mmol), and cesium iodide (80.0 mg, 0.306 mmol) were charged into a silica ampoule. The ampoule was cooled with liquid nitrogen and then sealed under static vacuum. The ampoule was shaken to mix the contents, heated to 850 °C at a rate of 2 °C min^{-1}, maintained at 850 °C for 100 h, cooled to 400 °C at a rate of 0.2 °C min^{-1}, and then left at room temperature. A crude product containing metallic crystals and colorless solid was washed with a large amount of water and then dried in air. Yield of [**3**]: 45.2 mg (89%). The X-ray fluorescence spectrum showed that Tc, Se, and I were included in this solid. A single crystal suitable for X-ray analysis was selected from the high-temperature reaction mixture. The X-ray powder diffraction pattern of this sample agreed with the simulated pattern of single-crystal X-ray diffraction analysis.

$[Tc_6Te_{15}]$ ([4]): Technetium metal (10.4 mg, 0.105 mmol) and elemental tellurium (133.7 mg, 1.05 mmol) were charged into a silica ampoule and sealed under static vacuum. The ampoule was shaken to mix the contents, heated to 900 °C at a rate of 2 °C min^{-1}, maintained at 900 °C for 248 h, cooled to 0.2 °C min^{-1} to 400 °C, and then left at room temperature. The metallic crystalline product was separated from the unreacted tellurium by hand. Yield of [**4**]: 26.5 mg (60%). The X-ray fluorescence spectrum showed that Tc and Te were included in this solid. A single crystal suitable for X-ray analysis was selected from the reaction mixture. The X-ray powder diffraction pattern of this sample agreed with the simulated pattern obtained by single-crystal X-ray diffraction analysis.

X-ray Crystallographic Determinations: Respective crystal of Cs_4[**1**]·CsBr, [**3**], and [**4**] were sealed in thin-walled glass capillaries. The data were collected with a Rigaku AFC-7R or an AFC-5R diffractometer at 296 K. The cell parameters were obtained by least-squares refinement of 25 reflections. All of the data were corrected for Lorentz and polarization effects, and Ψ scans were applied. Crystal decomposition did not occur during data collection. The structures were determined by direct methods, and the positional and thermal parameters of the non-H atoms were refined anisotropically by the full-matrix least-squares method. All of the calculations were performed by using TEXSAN.[40] Crystallographic details for Cs_4[**1**]·CsBr, [**3**], and [**4**] are gathered in Table 2. Further details of the crystal-structure investigations may be obtained from the Fachinformationszentrum Karlsruhe, 76344 Eggenstein-Leopoldshafen, Germany, on quoting the depository numbers CSD-421196, -421197, and -421198.

Table 2. Crystallographic data for Cs_4[**1**]·CsBr, [**3**], and [**4**].

	Cs_4[**1**]·CsBr	[**3**]	[**4**]
Formula	$Cs_5Tc_6S_8Br_7$	$Tc_6Se_8I_2$	Tc_6Te_{15}
Fw	2074.38	1467.49	2496.00
Crystal system	trigonal	monoclinic	orthorhombic
Space group	$R\bar{3}c$	$P2_1/n$	*Pbca*
a [Å]	9.962(1)	6.571(2)	14.237(2)
b [Å]	9.962(1)	11.998(2)	12.987(3)
c [Å]	54.70(1)	10.276(1)	12.917(2)
β [°]		99.67(1)	
V [Å^3]	4701(1)	798.7(2)	2388.4(7)
Z	6	2	4
$D_{calcd.}$ [g cm^{-3}]	4.370	6.102	6.941
T [K]	296.2	296.2	296.2
μ [mm]	17.75	27.06	21.29
R_1[a]	0.032	0.039	0.072
R_w[b]	0.091	0.111	0.181
GOF	1.04	0.91	1.09

[a] $R_1 = \Sigma||F_o| - |F_c||/\Sigma|F_c|$. [b] $R_w = \{\Sigma[w(F_o^2 - F_c^2)^2/\Sigma[w(F_o^2)^2]\}^{1/2}$.

Other Measurements: UV/Vis spectra were recorded with a Jasco V-550 spectrophotometer. Elemental analyses of C and H were carried out with a Yanaco MT-3 analyzer. Elemental analysis of Tc was carried out by measuring radioactivity with a Beckman LS 6500 liquid scintillation counter. X-ray fluorescence spectra were recorded with a Seiko Instruments SEA-2001. The X-ray powder diffraction pattern of insoluble [**3**] and [**4**] were collected with a Rigaku RAD-IC diffractometer by using Cu-K_α radiation (1.54178 Å) with a scan rate of 1° min^{-1} ($5 \leq 2\theta \leq 60°$). To prevent dispersion of radioactive materials, polycarbonate-coated samples were used, which were obtained by drying the suspensions in polycarbonate/chloroform on glass plates. Cyclic voltammetry (CV) measurements were performed with a Hokuto Denko HABF1510m potentiostat with an X–Y recorder at room temperature by using a scan rate of 100 mV s^{-1}. The working and counter-electrodes were a glassy carbon (ϕ = 1 mm) and a platinum wire, respectively. Sample solutions (1 mM) in 0.1 M $(Bu_4N)PF_6/CH_3CN$ were deoxygenated by an argon stream. The reference electrode was Ag/AgCl, for which the half-wave potential of ferrocene/ferrocenium (Fc/Fc^+) in CH_3CN was +0.43 V.

Supporting Information (see footnote on the first page of this article): Method used to prepare the solid containing $Cs_2[Tc_6Se_8Br_4]$ and a figure showing the ORTEP diagram of $Cs_2[Tc_6Se_8Br_4]$.

Acknowledgments

We thank Dr. K. Minato, Dr. Y. Shirasu, Dr. I. Nishinaka, and Dr. Y. Nagame of Japan Atomic Energy Agency for giving us the technetium metal as a gift. We are grateful to Prof. Y. Sasaki of Hokkaido University and Dr. Y. V. Mironov of Siberian Branch of Russian Academy of Science for their valuable discussions.

[1] A. Perrin, C. Perrin, *J. Cluster Sci.* **2009**, *20*, 1–7.
[2] Z. Zheng, X. Tu, *CrystEngComm* **2009**, *11*, 707–719.
[3] V. E. Fedorov, Y. V. Mironov, N. G. Naumov, M. N. Sokolov, V. P. Fedin, *Russ. Chem. Rev.* **2007**, *76*, 529–552.
[4] Y. Sasaki, *Bull. Jpn. Soc. Coord. Chem.* **2006**, *48*, 50–58.
[5] Y. Sasaki, *J. Nucl. Radiochem. Sci.* **2005**, *6*, 145–148.
[6] H. D. Selby, Z. Zheng, *Comments Inorg. Chem.* **2005**, *26*, 75–102.
[7] E. J. Welch, J. R. Long in *Progress in Inorganic Chemistry* (Ed.: K. D. Karlin), Wiley, New York, **2005**, vol. 54, pp. 1–45.
[8] H. D. Selby, B. K. Roland, Z. Zheng, *Acc. Chem. Res.* **2003**, *36*, 933–944.
[9] T. G. Gray, *Coord. Chem. Rev.* **2003**, *243*, 213–235.
[10] J.-C. P. Gabriel, K. Boubekeur, S. Uriel, P. Batail, *Chem. Rev.* **2001**, *101*, 2037–2066.
[11] T. Saito, *J. Chem. Soc., Dalton Trans.* **1999**, 97–106.
[12] A. Perrin, M. Sergent, *New J. Chem.* **1988**, *12*, 337–356.
[13] A. Perrin, C. Perrin, M. Sergent, *J. Less-Common Met.* **1988**, *137*, 241–265.
[14] E. G. Tulsky, J. R. Long, *Inorg. Chem.* **2001**, *40*, 6990–7002.
[15] K. Ramaswamy, E. G. Tulsky, J. R. Long, J. L. F. Kao, S. E. Hayes, *Inorg. Chem.* **2007**, *46*, 1177–1186.
[16] W. Bronger, M. Kanert, M. Loevenich, D. Schmitz, *Z. Anorg. Allg. Chem.* **1993**, *619*, 2015–2020.
[17] W. Bronger, M. Kanert, M. Loevenich, D. Schmitz, K. Schwochau, *Angew. Chem. Int. Ed. Engl.* **1993**, *32*, 576–578.
[18] V. I. Spitsin, S. V. Kryuchkov, M. S. Grigoriev, A. F. Kuzina, *Z. Anorg. Allg. Chem.* **1988**, *563*, 136–152.
[19] S. V. Kryuchkov, A. F. Kuzina, V. I. Spitsin, *Z. Anorg. Allg. Chem.* **1988**, *563*, 153–166.
[20] K. E. German, S. V. Kryutchkov, *Russ. J. Inorg. Chem.* **2002**, *47*, 578–583.
[21] J. Lu, M. J. Clarke, C. D. Hiller, *Inorg. Chem.* **1993**, *32*, 1417–1423.
[22] J. Baldas, S. E. Colmanet, G. A. Williams, *Aust. J. Chem.* **1991**, *44*, 1125–1132.
[23] M. S. Grigoriev, S. V. Kryutchkov, *Radiochim. Acta* **1993**, *63*, 187–193.
[24] M. S. Grigoriev, A. A. Miroslavov, G. V. Sidorenko, Y. T. Struchkov, D. N. Suglobov, A. I. Yanovskii, *Radiochemistry* **1995**, *37*, 177–179.
[25] M. S. Grigoriev, A. E. Miroslavov, G. V. Sidorenko, D. N. Suglobov, *Radiochemistry* **1997**, *39*, 202–204.
[26] V. E. Fedorov, N. V. Podberezskaya, A. V. Mishchenko, G. F. Khudorozhko, I. P. Asanov, *Mater. Res. Bull.* **1986**, *21*, 1335–1342.
[27] J. R. Long, L. S. McCarty, R. H. Holm, *J. Am. Chem. Soc.* **1996**, *118*, 4603–4616.
[28] A. Slougui, S. Ferron, A. Perrin, M. Sergent, *Eur. J. Solid State Inorg. Chem.* **1996**, *33*, 1001–1013.
[29] S. S. Yarovoi, S. F. Solodovnikov, Y. V. Mironov, V. E. Fedorov, *J. Struct. Chem.* **2003**, *44*, 318–321.
[30] G. Pilet, A. Perrin, *Solid State Sci.* **2004**, *6*, 109–116.
[31] T. Yoshimura, K. Umakoshi, Y. Sasaki, A. G. Sykes, *Inorg. Chem.* **1999**, *38*, 5557–5564.
[32] Z. Zheng, T. G. Gray, R. H. Holm, *Inorg. Chem.* **1999**, *38*, 4888–4895.
[33] N. Lepareur, F. Mevellec, N. Noiret, F. Refosco, F. Tisato, M. Porchia, G. Bandoli, *Dalton Trans.* **2005**, 2866–2875.
[34] L. E. Helberg, S. D. Orth, M. Sabat, W. D. Harman, *Inorg. Chem.* **1996**, *35*, 5584–5594.
[35] J. Barrera, A. K. Burrell, J. C. Bryan, *Inorg. Chem.* **1996**, *35*, 335–341.
[36] J. V. Caspar, B. P. Sullivan, T. J. Meyer, *Inorg. Chem.* **1984**, *23*, 2104–2109.
[37] B. E. Wilcox, E. Deutsch, *Inorg. Chem.* **1991**, *30*, 688–693.
[38] T. Takahira, K. Umakoshi, Y. Sasaki, *Chem. Lett.* **1994**, 2315–2318.
[39] A. W. Maverick, J. S. Najdzionek, D. MacKenzie, D. G. Nocera, H. B. Gray, *J. Am. Chem. Soc.* **1983**, *105*, 1878–1882.
[40] TEXSAN. *Single-Crystal Structure Analysis Package*, Molecular Structure Corp., Woodlands, TX, **1992**.

Received: November 2, 2009
Published Online: February 10, 2010

